EUROPEAN ORGANIZATION FOR NUCLEAR RESEARCH
CERN - ACCELERATORS AND TECHNOLOGY SECTOR

CERN-ATS-2012-057

Performance Improvement of a Measurement Station for Superconducting Cable Test

P. Arpaia[1,2], L. Bottura[2], G. Montenero[1,2], S. Le Naour[2]

1 Engineering Department, University of Sannio, Benevento, Italy
2 CERN, Geneva, Switzerland

Abstract

A fully digital system, improving measurements flexibility, integrator drift, and current control of superconducting transformers for cable test, is proposed. The system is based on a high-performance integration of Rogowski coil signal and a flexible direct control of the current into the secondary windings. This allows state-of-the-art performance to be overcome by means of out-of-the-shelf components: on a full-scale of 32 kA, current measurement resolution of 1 A, stability below 0.25 $Amin^{-1}$, and controller ripple less than 50 ppm. The system effectiveness has been demonstrated experimentally on the superconducting transformer of the Facility for the Research of Superconducting Cables at the European Organization for Nuclear Research (CERN).

Submitted to "Review of Scientific Instruments"

Geneva, Switzerland

March 2012

Performance improvement of a measurement station for superconducting cable test

Pasquale Arpaia,[1,2] Luca Bottura,[2] Giuseppe Montenero,[1,2] Sandrine Le Naour[2]

[1]*Engineering Department, University of Sannio, 82100 Benevento, Italy.*

[2]*European Organization for Nuclear Research (CERN), 1217 Geneva, Switzerland*

A fully digital system, improving measurements flexibility, integrator drift, and current control of superconducting transformers for cable test, is proposed. The system is based on a high-performance integration of Rogowski coil signal and a flexible direct control of the current into the secondary windings. This allows state-of-the-art performance to be overcome by means of out-of-the-shelf components: on a full-scale of 32 kA, current measurement resolution of 1 A, stability below 0.25 $Amin^{-1}$, and controller ripple less than ±50 ppm. The system effectiveness has been demonstrated experimentally on the superconducting transformer of the Facility for the Research of Superconducting Cables at the European Organization for Nuclear Research (CERN).

I. Introduction

Superconductivity is a technology with a declared interest in several fields of physics and engineering [1]. A key design parameter for any large-scale application of superconductivity is the current carrying capacity, also referred to as “critical current”. Its assessment needs first and foremost for an accurate measurement of the voltage-current characteristic of the sample, in general, function of temperature, current, and magnetic field [2]. This is a relatively delicate task for single wires, nowadays carried out through quasi-industrial standards. On the other hand, for large-size cables, facilities of appropriate dimensions and functionality are few, mainly owing to the difficulty and cost of providing a large and complex set-up for assessing the device properties as a function of the abovementioned parameters [3-8].

Cable critical current tests commonly involve current levels in the order of the tens of kA, in principle supplied by large power converters. However, main drawbacks are significant equipment cost, and the need for large current leads, resulting in high cryogenic loads and operating costs. For this reason, in this range of current, an interesting alternative is

to use superconducting transformers [9-17]. A low current is fed to a superconducting primary winding with a large number of turns, inductively coupled to a superconducting secondary with a much smaller number of turns and directly connected to the sample under test. The modest primary current, usually in the range of 100 A, can be generated with relatively inexpensive and standardized power supplies, and the current feed-through into the cryogenic environment can be optimized to have lower cryogenic load by orders of magnitude. Such a device provides test capability at moderate capital and operating cost.

Beyond the obvious issues on the performance and protection of the primary and secondary windings, one of main concerns in the operation of a superconducting transformer for cable test is a suitable control, with a precise and accurate measurement of the secondary current. Indeed, current measurement is a key component of the control loop. Resistive losses due to the interconnections between the secondary and the sample lead to an unavoidable decay of current, unless the primary current is adjusted continuously to compensate and maintain the sample current at the desired set value. The control loop, on the other hand, must account for the physical characteristics of the coupled system formed by the primary winding, and its power supply, the secondary, and the current transducer.

In [10] and [11], advanced systems for measuring the secondary current and for compensating its decay are proposed. Both are based on similar concepts for the improvement of the current measurement quality and the implementation of a suitable control. The sensing elements for the current are two Rogowski coils connected in anti-series, providing a good rejection to parasitic couplings. The transducer signal is integrated in time by using digital integrators, and the integral is converted to current by means of a suitable calibration coefficient. The signal conditioning and the control are then implemented by means of customized analog electronics. In [10], main drawbacks are the resolution and the offset of the digital integrator. In [11], these issues are addressed both by implementing a custom FPGA-based integrator with higher resolution and by minimizing the residual offset via a dedicated procedure. However, the control loop is still analog (proportional action). Furthermore, in both the systems, instead of directly monitoring the secondary current, a voltage produced via a function generator is used as reference signal on the primary power supply, by giving rise to an indirect control strategy. This makes rather complex both the common operation of defining an arbitrary cable current cycle and the detection of system faults: a test cycle defined in terms of secondary current has to be converted in a corresponding voltage. This requires that the closed-loop transfer function is known with satisfying accuracy for all the operating conditions.

In this paper, a flexible system improving the state-of-the-art of superconducting cable testing based on transformers is proposed to overcome state-of-the-art solution by meeting the overall target of a secondary current control for a 32 kA full range, with resolution better than 3 A, relative ripple less than 10^{-4}, and stability below 0.5 $Amin^{-1}$. The secondary current measurement is improved by compensating the residual offset of a high-performance digital integrator by adjusting the self-calibration time. The measurement system is integrated in a fully-digital control loop, with all the related benefits [18], i.e. good noise margins, easiness in the implementation/modification, and so on. In particular, in Section 2, the proposed measurement system with the associated digital control algorithm is illustrated. In Section 3, experimental results from the on-field characterization and validation of the proposed system at CERN, in the Facility for Research on Superconducting Cables (FReSCa) [4] are illustrated.

II. The Proposed System

In Fig. 1, the architecture of a measurement station for superconducting cable test, based on a transformer for supply and Rogowski coils for current measurement, is reported. The objective is to generate a test current in the sample I_s, i.e. in the transformer secondary, ideally equal to the set point I_{ref}. At this aim, the main issue is to provide a direct control of the secondary current I_s. The control block, according to the feedback signal I_m from the measurement system, acts to provide a reference voltage V_{ref} to the power supply of the primary, a voltage-controlled current source. The source drives the current I_p into the primary, by inducing a secondary current I_s. In turn, I_s is sensed by means of two Rogowski coils, suitably positioned in phase opposition and connected in anti-series in order to reject parasitic electromagnetic couplings to stray fields. The coils voltage signal V_{RC} is proportional to the secondary current rate dI_s/dt. The secondary current is then obtained by integrating the differential signal V_{RC} from the Rogowski coils. The measured current is finally compared to the reference I_{ref} in order to generate the feedback signal I_m compensating for resistive losses.

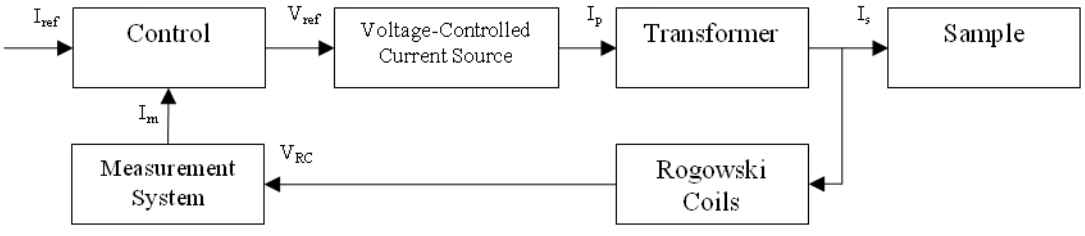

FIG. 1. Architecture of a transformer-based measurement station for superconducting cable test.

In this architecture, the fundamental elements are the measurement system and the control strategy. The former has to provide high-quality measurements, by minimizing undesired uncertainty effects, such as integrator drift and noise. The latter has to follow closely the reference signal, i.e. the desired secondary current I_s, by accurately driving the current into the primary I_p. Moreover, the overall system should be flexible, in order to allow quick modifications of the desired waveforms according to the test needs.

The above-mentioned requirements are met by exploiting high-performance numerical integration and digital control algorithms, as described below.

A. The measurement and control system

In Fig. 2a, the architecture of the measurement and control system is shown. The control reference V_{ref} is generated by a digital waveform generator, with at least 16 bits of resolution in the input range of the voltage-controlled current source (Fig. 2b) in order to accurately control I_p. The Rogowski coils signal V_{RC}, acquired by means of a digital integrator, is related to the secondary current in the ideal case as:

$$V_{RC} = K_{RC} \frac{dI_s}{dt} \quad (1)$$

where K_{RC} (VsA^{-1}) is the sensitivity coefficient of the Rogowski coils in anti-series configuration. Then, after digital integration, the measured magnetic flux is:

$$\Phi_{Meas}(n) = K_{RC} I_s(n) + \Phi_{offset}(n) \quad (2)$$

where n stands for a discrete time instant, and $\Phi_{offset}(n)$ is the undesired flux contribution arising from the voltage offset on the data acquired from the integrator. This integration equivalent offset signal arises from both all the circuit before the integrator input as well as from the integrator itself. In practice, design objectives are achieved by imposing the following requirements on the integrator:

- Signal-to-Noise Ratio (SNR) better than 90 dB, for resolution in current readings better than 1 A on a full-scale of 32 kA;

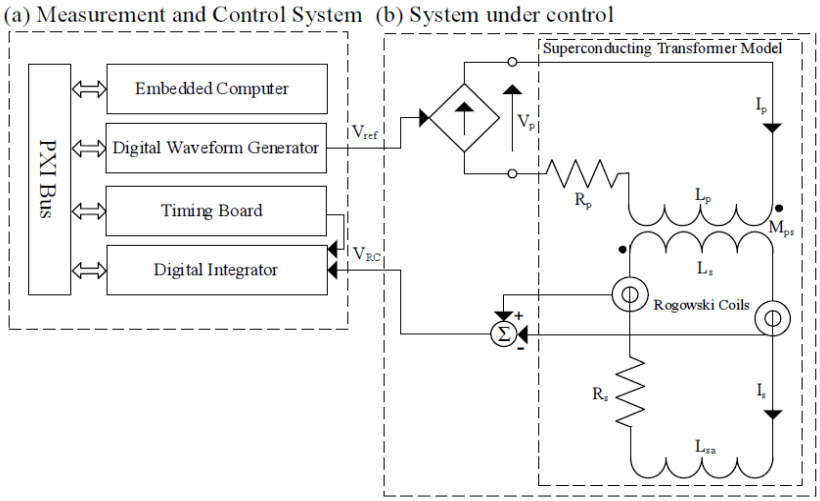

FIG. 2. Architecture of (a) measurement and control system, and (b) system under control.

- stability better than ±10 ppm on 24 hours, for effective offset correction.

Other requirements of EMC noise rejection, thermal stability, data throughput, and timing signals accuracy are met by an advanced measurement bus (e.g. PXI) with embedded controller [19].

Finally, a timing board allows signals among instruments to be synchronized, with accuracy suitable for the desired trigger.

Beyond well-known advantages of a fully digital measurement, the proposed architecture allows off-the-shelf boards, advanced digital signal processing, and software flexibility to be exploited. Moreover, a software control algorithm can be implemented if the sampling frequency is less than few hundreds of samples/s.

B. The system under control

The superconducting transformer is modeled as a resistive air-core transformer [20] (Fig. 2b):

$$\begin{cases} V_p + M_{ps}\frac{dI_s}{dt} = I_p R_p + L_p \frac{dI_p}{dt} \\ M_{ps}\frac{dI_p}{dt} = I_s R_s + (L_s + L_{sa})\frac{dI_s}{dt} \end{cases} \quad (3)$$

where V_p is the primary voltage, M_{ps} the mutual between primary and secondary, R_p the primary resistance, mainly due to resistive current leads, L_p the primary inductance, R_s the secondary resistance, mainly due to the electrical junctions in the secondary circuit, L_s the secondary inductance, and L_{sa} the sample inductance. The first eq. of (3) provides the dependence of the currents on the voltage V_p, and the second eq. of (3) provides the link between primary and secondary currents.

From (3) the transformer transfer function is derived using the Laplace transform:

$$H_T(s) = \frac{I_s(s)}{I_p(s)} = G_T \frac{s}{s+\frac{1}{\tau}} \quad (4)$$

where G_T is the transformer gain, i.e. the current amplification factor, without losses (R_s=0) $G_T = \frac{M_{ps}}{L_p+L_{sa}}$, and τ the decay time constant of I_s, $\tau = \frac{L_p+L_{sa}}{R_s}$. The (4) justifies the need for a control strategy to counteract the resistive current decay in the secondary circuit [21].

The ideal values of the parameters in (4) can be easily calculated in the linear case, i.e. by neglecting dependence on the current and on any dia- or ferro-magnetic effects. However, according to [12,13], the joint resistance and the self-inductance are a function of the current and the field. Moreover, the sample inductance can differ from its nominal value [11]. These effects lead the parameters of the controlled circuit to deviate from theory, giving rise to non-linearity to be accommodated in the control system.

C. Digital control algorithm

In [10] and [11], an indirect control scheme is realized by means of mainly a voltage function generator and customized electronics. Conversely, in this work, a fully digital measurement system and control algorithm, taking into account only the *plant* characteristic without further analog signal handling, is proposed.

In Fig. 3, the diagram of the proposed one-degree feedback controller is shown. The following assumptions are made:

- The symbols * and z refer to signals in discrete-time and *z*-transform domains, respectively.
- A discrete Proportion-Integral algorithm *PI(z)* is chosen for its simple implementation, tuning, and robustness.
- The digital-to-analog conversion of the digital waveform generator is modeled by a discrete-to-continuous time conversion (*n/t*).
- The voltage-controlled current source is modeled as a pure gain G_{PS}, provided that the sampling period T_s, triggered from the timing board, is larger than the characteristic time constant of the power supply. This provides an accurate conversion of the reference voltage V^*_{ref} into the primary current I_p.
- The transformer is modeled according to (4).
- The measurement of the current I_s is considered ideal (uncertainty is considered in Sec. III).

- The conversions *n/t* and *t/n* are equivalent to Zero-Order Holder Filtering (ZOH).

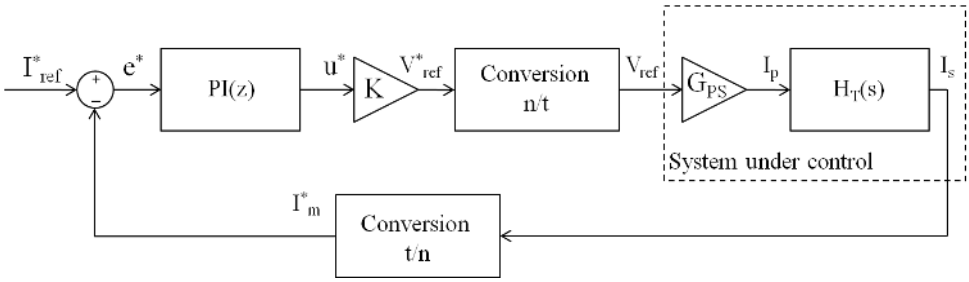

FIG. 3. One-degree feedback controller for superconducting transformer.

1. Design of Proportional-Integral digital controller

The design follows standard practice by aiming at a suitable choice of the controller parameters. The transfer function of the Proportional-Integral controller *PI(z)* can be written for a backward digital integrator as:

$$PI(z) = K_P + K_I \frac{z}{z+1} \tag{5}$$

where K_P and K_I are the gains of the proportional and integral actions, respectively. The gain K (Fig. 3) is the transduction constant from the output u^* to V^*_{ref}, in turn related to the error signal e^*:

$$V^*_{ref}(z) = KPI(z)e^* \tag{6}$$

The desired current in the transformer secondary I^*_{ref} is related to the measured current I^*_m:

$$I^*_m(z) = H_{CL}(z)I^*_{ref} \tag{7}$$

where H_{CL} is the closed-loop transfer function:

$$H_{CL}(z) = \frac{KG_{PS}PI(z)H_T(z)}{1+KG_{PS}PI(z)H_T(z)} \tag{8}$$

$H_T(z)$ is obtained by z-transforming the product of the transformer transfer function (4) by a ZOH with sample period T_s:

$$H_T(z) = G_T \frac{z-1}{z-e^{-T_S/\tau}} \tag{9}$$

The sample period depends on the required bandwidth, customarily set to 5 to 20 times the inverse of the maximum allowed frequency. The value of K is calculated according to the final-value theorem. By assuming (i) open-loop operation, and (ii) an input current step $U(z)=z/(z-1)$ with amplitude $I_{s,max}$, the steady-state response for V^*_{ref} is:

$$\lim_{n\to\infty} V^*_{ref}(n) = \lim_{z\to 1} \frac{z-1}{z} KPI(z)I_{s,max}\,U(z) = KI_{s,max}(K_I + K_P) \tag{10}$$

where $I_{s,max}$ is assumed as the maximum quench current of the transformer secondary winding. Then, K is calculated by imposing the (10) does not exceed the voltage $V^*_{ref,max}$ required to power the primary with the maximum allowed current $I_{p,max}$:

$$K = \frac{V_{ref,max}}{I_{s,max}(K_I+K_P)} = \frac{I_{p,max}}{G_{PS}I_{s,max}(K_I+K_P)} \quad (11)$$

The (11) depends on K_P and K_I, determined by tuning the response of the controllers. But (K_P + K_I) can be limited by applying the reaction-curve method [18], i.e. by defining reasonable slope and steady-state gain for the step response. Moreover, the value defined in (11) can be lowered by assuming a margin of 2 % on the maximum of the primary current. This allows the $I_{p,max}$ to be not attained, because that can lead to a quench of the primary.
By substituting $PI(z)$ and $H_T(z)$, the expression of the closed-loop transfer function is:

$$H_{CL}(z) = \left(\frac{KG_{PS}G_T(K_I+K_P)}{1+KG_{PS}G_T(K_I+K_P)}\right)\frac{z-\left[\frac{K_P}{(K_I+K_P)}\right]}{z-\left[\frac{KG_{PS}G_TK_P+e^{-T_S/\tau}}{1+KG_{PS}G_T(K_I+K_P)}\right]} \quad (12)$$

The (12) represents a first-order filter with behavior defined by the pole position inside the unit circle. The zero depends on K_P and K_I. By further imposing a convenient proportionality $K_I=mK_p$, the zero is in the form $1/(1+m)$. The pole must be chosen so that the desired signal bandwidth can pass through the filter. The knowledge of the range of the transformer transfer function parameters allows the effect of positioning the pole along the real axes to be verified. Under the assumptions of ideality, the (12) also demonstrates intrinsic stability.

III. Experimental Results

The proposed system was tested at CERN, on FReSCa, the Facility for Research on Superconducting Cables [4]. The FReSCa set-up includes: (i) two coaxial cryostats, independently cooled either at 4.3 or at 1.9 K, (ii) a background-field magnet, housed in the outer cryostat, with a maximum field of 10.3 T, and (iii) a sample insert, either or connected to an external room-temperature 32-kA power supply via copper current leads, self-cooled by the vapor from the 4.3 K-He bath, or including an assembly (Fig. 4a), with a superconducting transformer (Fig. 4b) [10], with maximum currents of 50 A in the primary and 38 kA in the secondary. The secondary current is measured by means of two Rogowski coils (Fig. 2), connected in anti-series, consisting of about 2600 turns of 0.2-mm copper wire, with the characteristics of Tab. I.

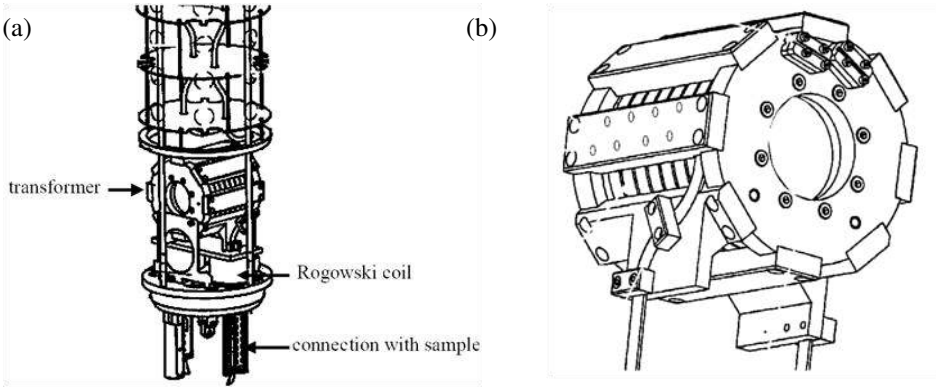

FIG. 4. The sample insert (a) and the superconducting transformer (b) of FReSCa at CERN.

The primary winding of the transformer is wound from insulated NbTi wire, with a diameter of 0.542 mm, a Cu/SC (Copper to Superconducting) ratio of 1.35, a residual resistivity ratio of 82, and a filament diameter of 45 μm. The primary has a solenoid shape, with a height of 160 mm, and inner and outer radii of 70 and 88 mm, respectively. The coil has 33 layers, with in total 10850 turns, and an inductance of 11.75 H (L_p). The secondary winding is wound directly over the primary, and consists of 7 turns of a NbTi-Rutherford cable with a width of 15.1 mm. The secondary is impregnated with epoxy to support mechanically the coil. All along the cable, a copper strip thick 1 mm is soldered for mechanical and electro-dynamical stability. The self-inductance of the secondary is 9 μH (L_s) and the mutual inductance between primary and secondary is 8.77 mH (M_{ps}).

TABLE.I Rogowski Coil Parameters.

coil height	70	(mm)
coil inner radius	27	(mm)
coil outer radius	56	(mm)
material of the core	(G10)	
material of the wire	copper	
wire diameter	0.2	(mm)
number of turns	About 2600	
number of layers	6	

In the following, (A) the *experimental set-up*, (B) the *controller parameters determination*, (C) the *measurement system characterization*, and (D) the *validation results* of the proposed system are described.

A. Experimental Set-Up

In Fig. 5, the measurement and control setup is shown. The waveform generator is realized through a data acquisition board NI-PXI 6281 of National Instruments [22].

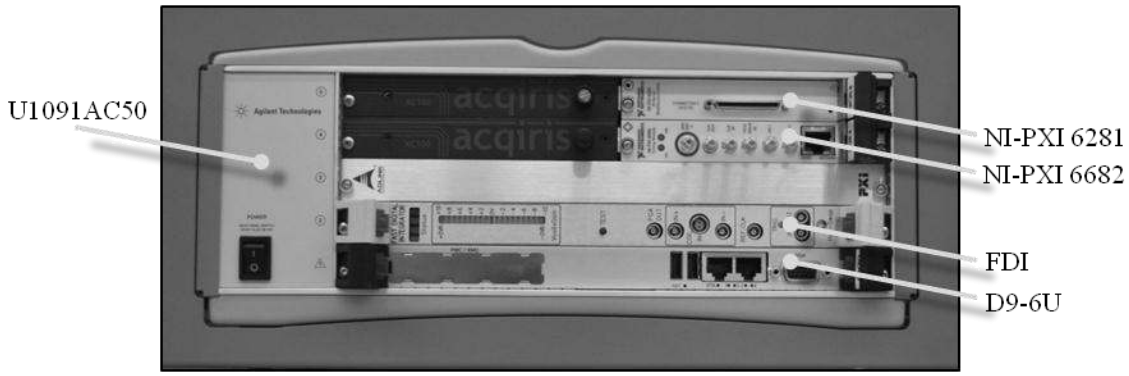

FIG. 5. Measurement and control setup.

This multifunctional board provides also digital I/O, for interfacing the standard FReSCa quench protection and data acquisition systems [23], and analog inputs in the range of ±1 V, with a resolution of 30 μV, for the system characterization. The board drives a four-quadrants power supply Lake Shore Mod 622 [24], supplying the transformer's primary (voltage-controlled current source in Fig. 1). The ideal gain of the power supply is 100 AV^{-1}, with voltage ranges of ±1 V and ±5 V, in input and output, respectively.

The core of the system is the Fast Digital Integrator (FDI) [25] for the transformer's secondary current measurements via the signal from the Rogowski coils. The signal-to-noise and distortion ratio is higher than 100 dB. Typical static non-linearity, relative to a full scale of ±10 Vs and with temperature ranging between 27 and 35 °C, is within ±7 ppm. The transfer function has typical relative errors of 0.2 % for the gain and 17 ppm (on the full scale) for the offset. Typical stability is ±1 ppm over 30 minutes at 30 °C.

The timing board is a NI PXI-6682 of National Instruments, with 10 MHz of internal clock [26], used to generate the trigger signal for the FDI and for the data acquisition board.

The boards are housed in an PXI crate U1091AC50 by Agilent [27]. The embedded computer is a Single-Board Computer D9-6U by Mikro Elektronik [28], hosting the software handling the whole system functions, based on the Flexible Framework for Magnetic Measurements [29], and implementing the controller algorithm.

B. Controller parameters determination

Defining the largest required signal bandwidth for the secondary current enables to specify the sample frequency of the closed-loop operation and thereafter the controller parameters.

The bandwidth is determined by assuming a triangular reference signal with maximum allowed slope, and a current equal to the minimum required for operation. The maximum current ramp rate in the secondary is set to 800 As^{-1} in order to not reach the voltage limit (± 5 V) across the power supply on the primary, (see (3)). For a minimum current I_s of 500 A in the transformer, i.e. a reasonable lower bound for the test of a cable with critical current in the range of several tens of kA, the signal bandwidth B at 95 % is around 4 Hz [30]. In practice, this value can be thought much lower because for testing purposes the current has smooth transition to the maximum ramp-rate. In this case, a sample rate f_s of 20 S/s is a suitable choice: 5 times the bandwidth B and a sample period 5 times higher than the characteristic time constant of the power supply. The required numeric bandwidth for the control is therefore 0.2 (B/f_s).

Once the sample rate is defined, the controller parameters K, K_I, and K_P can be calculated [18]. According to the reaction curve method, a trade-off for the controller gains is $K_I + K_P = 10$. As the required bandwidth is 0.2, and taking into account the relation $K_I = mK_p$, the proportional and integral gains can be calculated as $K_P = K_I = 5$ (with $m=1$). By assuming $I_{s,max}$ to be 36 kA (slightly lower than the maximum quench current reached by the transformer) in (11), K is $1.36 \cdot 10^{-6}$ VA^{-1}.

In Figs. 6, the bounds of the frequency response of the closed-loop transfer function (12), using ideal G_T and τ are illustrated for a typical variation of ±30 % of the transfer function parameters (namely, left, the magnitude, and, right, the phase).

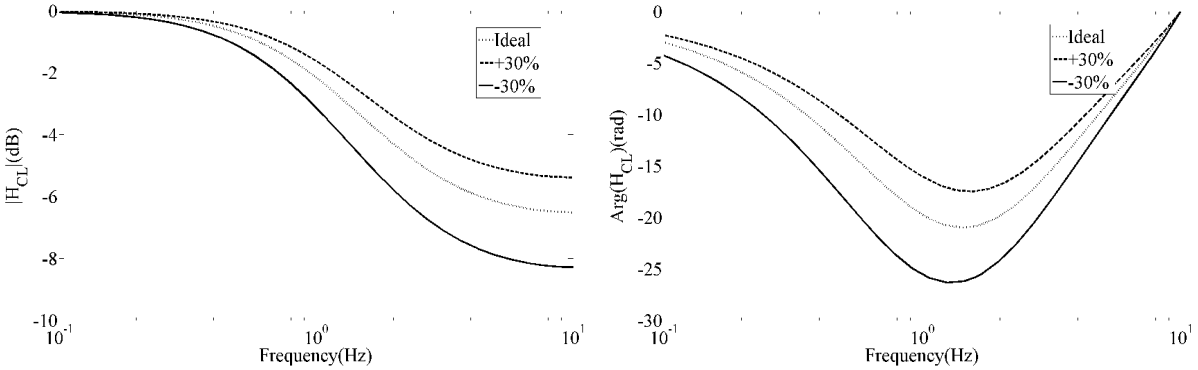

FIG. 6. Frequency response bounds of the closed-loop transfer function (12), with ideal G_T and τ, for a typical variation of ±30 % of the transfer function parameters (left, magnitude, and, right, phase).

The zero of the transfer function is 0.5 and the pole is placed around 0.7. With the taken values of G_T and τ the filter behaves as a low-pass. The -3 dB bandwidth is about 2 Hz. This value can be easily increased by f_s higher than 20 S/s (e.g. for f_s=60 S/s the -3 dB

bandwidth is 5 Hz); however, such as shown in next Section, this value of 20 S/s is suitable for the required performance.

C. Measurement System Characterization

Main problems in the secondary current measurement arise from the integration equivalent offset and from the repeatability of Rogowski Coils in typical test conditions.

The integration equivalent offset depends on the procedure for its correction. Moreover, as the same integrator is used for the calibration of the Rogowski coils, the offset affects also the sensitivity coefficient K_{RC}. The offset contribution was minimized by averaging the samples for 1 min before each measurement and by subtracting the average from the measurement results.

Repeatability is mainly affected by mutual coupling between Rogowski coils and transformer's primary[9,10]. In the following, the experimental analysis of repeatability and stability during a long test of several minutes for the system composed by Rogowski coils and integrator are described. Tests were carried out in a special sample configuration (Figs. 7), by closing the insert directly on a short superconducting circuit, obtained by means of a NbTi dipole inner layer cable of the Large Hadron Collider (LHC). An open-loop measurement (i.e. without activating the feedback control system) was configured in order to minimize the impact of other factors related to the specific sample under test.

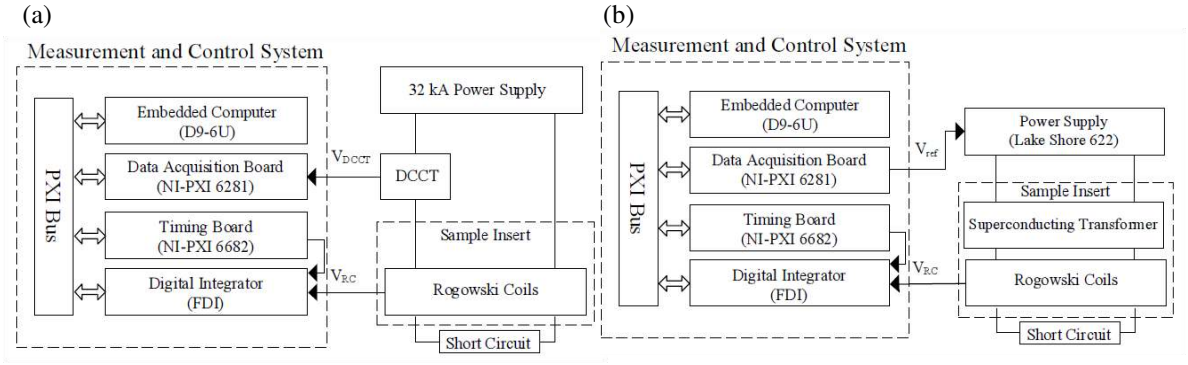

FIG. 7. Set up for the measurement system characterization: (a) repeatability and (b) stability tests.

1. Repeatability

For the repeatability tests of the system composed by the Rogowski coils and FDI, the sample was fed directly from the room-temperature 32-kA power supply, through large current leads (Fig. 7a). The two Rogowski coils were located inside the sample insert, analogously as in the

superconducting transformer insert (Fig. 4). The reference was provided by the direct-current current transformer (DCCT) of the 32-kA power supply.

The repeatability was assessed as the standard deviation of the sensitivity coefficient K_{RC} with the Rogowski coils coupled with the secondary, temperature 4.3 K, integrator gain 20, offset correction time of 1 min, and external field of 0.0 T. The DCCT and the Rogowski coils signals are acquired synchronously at 20 S/s, by means of the data acquisition board and the FDI, respectively, by ramping the current from 500 A to 10 kA, at different rates from 100 to 800 As^{-1}. K_{RC} is computed by dividing the calculated average voltage on 200 samples at the FDI input by the estimated ramp rate during the ramp up. The result is 58.40 μVsA^{-1} ± 0.06 %, in comparison to an ideal value of 58.68 μVsA^{-1}, and to a warm value of 58.07 μVsA^{-1} ± 0.1 %.

In Fig. 8, the 1-σ repeatability (200 samples) is analyzed at varying the current ramp rate. Tests were carried out with and without a field of 6 T in the magnet providing the background field, in order to verify a possible coupling between coils and magnet. The results are compatible; therefore, the influence of the external field is not significant. The repeatability improves as the ramp rate increases. This is because the SNR increases according to the ramp rate, as the signal at the FDI input is larger, while the noise level from the power supply controller action is constant in this range of currents and current ramp-rates.

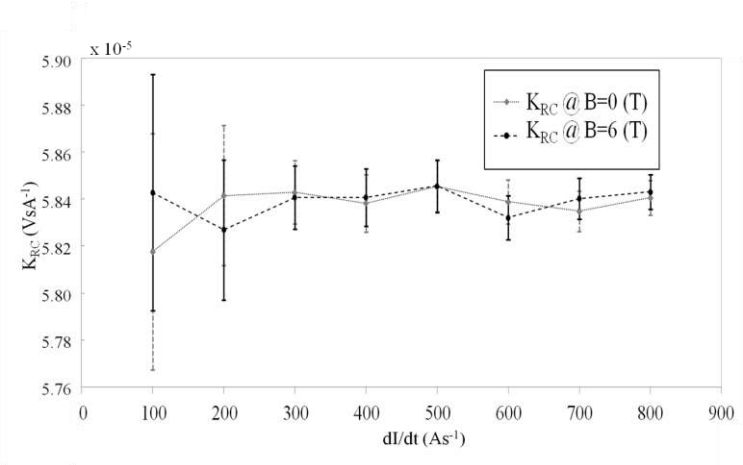

FIG. 8. 1-σ repeatability (200 samples) of the system Rogowski coils-integrators at varying the current ramp rate.

2. Stability

In Fig. 7b, the experimental set up for the stability tests of the measurement system is illustrated. The stability was assessed as the standard deviation in the difference between the initial and the final values of the measured current, during a closed powering cycle of long

duration (e.g. 10 min), divided by the time. The current, at the end of the cycles, is forced to zero by switching on the heaters on the transformer secondary, in order to push it into the resistive state. Therefore, the mismatch between initial and final values depends only on the measurement quality, and mainly on the residual integration equivalent offset.

The secondary current was measured on a set of 30 long cycles of 10 min, by achieving results in the range ±2 A (±0.15 %), corresponding to an average drift of ±0.18 $Amin^{-1}$. In Fig.9a, examples of four current measurements are shown. Open-loop cycles, composed by two ramps with nominal 50 A/s of rate, ascending/descending from 0.0 to 1.4 kA, were measured. In Fig.9b, details on the drift trend in terms of residual current are highlighted. These results are compatible with the design and the expected performance of FDI: a current drift of 0.25 $Amin^{-1}$ corresponds to 5.0 μV of equivalent offset of FDI, compatible with its stability specifications of ± 10 ppm over 24 hours. Such a very low drift is obtained also owing to the low noise generated by Rogowski coils at cryogenic temperature (below 5 K).

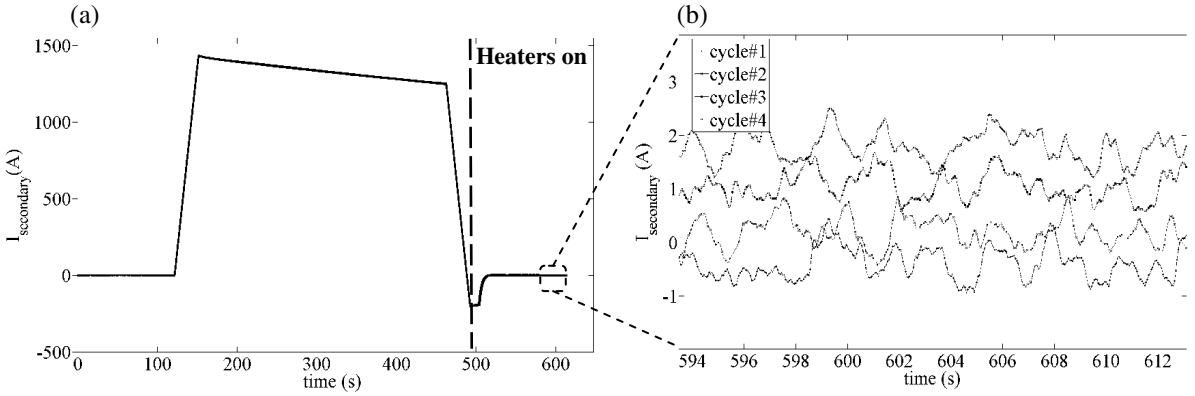

FIG. 9. Open-loop current cycles measured on the transformer secondary to assess the integration residual drift: (a) the whole cycles and (b) zoom on the end-cycles.

D. Validation Results

The above results do not point out the stability in actual on-field conditions, i.e. when the control loop is enabled. At this aim, the cable has to be powered by a long plateau close to its critical current: in such a condition, the sample shows a resistive behavior and the measured voltage across the cable will drift only if the current itself is drifting.

Thereafter, performance analysis was completed by validating the proposed system on the test chain as a whole, i.e. measurement and control loop, by two steps. In the first step, the controller performance was verified by studying the tracking of reference current waveforms in a configuration where the transformer insert is closed on a short circuit, analogously as in the measurement system characterization. The final step was the measurement of the voltage-

current curve of a reference superconducting cable. At this aim, a Rutherford NbTi cable with 36 strands of 0.825 mm diameter, used for the production of the outer layer of the LHC dipoles, the so-called LHC cable of type 2 [31], was employed.

1. Controller performance assessment

For a superconducting transformer control in a cable test facility, the tracking of the reference current during the ramp-up phase is a key factor. A linear ramp-up is suitable for a proper analysis of the measured voltage-current characteristic. For reasons of signal quality, a low current ripple due to controller action is mandatory, in order to keep the measured voltage noise level acceptable (few μV) on the measured sample.

The capability of the proposed control/measurement system was assessed by using the reference I_{ref} waveforms reported in Fig. 10, with the parameters summarized in Tab. II.

TABLE.II Setting of I_{ref} in the transformer's secondary in controller assessment (symbols in Fig. 10).

I_{max} (A)	I_{start} (A)	t_{start} (s)	Ramp Rate Up/Down (As^{-1})	t_{Imax} (s)	Acc=Dec (As^{-2})	I_{stop} (A)	t_{stop} (s)
500	0	2	300	10	200	0	10
10000	0	2	800	10	200	0	10
20000	0	2	800	10	200	0	10

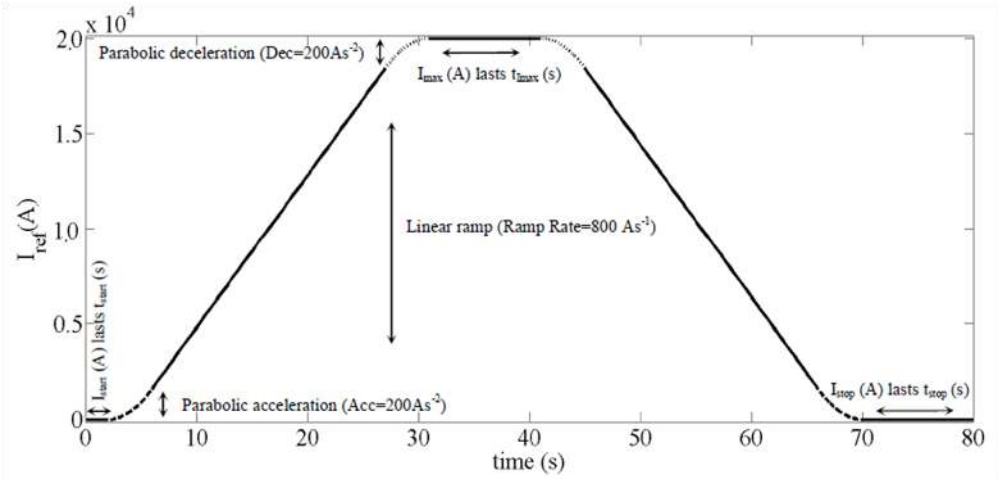

FIG. 10. Example of reference current curve I^*_{ref} in controller assessment tests.

Current ramp-rate acceleration and deceleration phases, implemented by parabolic functions, are identified by imposing the continuity of the derivative at the transition to a linear ramp [32]. These soft start/end curves avoid stepwise voltage spikes on the sample under test and provide a suitable control bandwidth. The controller was validated at the maximum ramp rate

(800 As^{-1}) for several values of maximum current, so to explore conditions of largest bandwidth and maximum variation for the transformer transfer function parameters.

In Fig. 11a, an example of the measured current I^*_m is compared to I^*_{ref} for the cycle at 20 kA. In Figs. 11b1 and 11b2, the differences between the measured current and the ideal linear reference at ramp up and its average value at the flattop, respectively, are detailed.

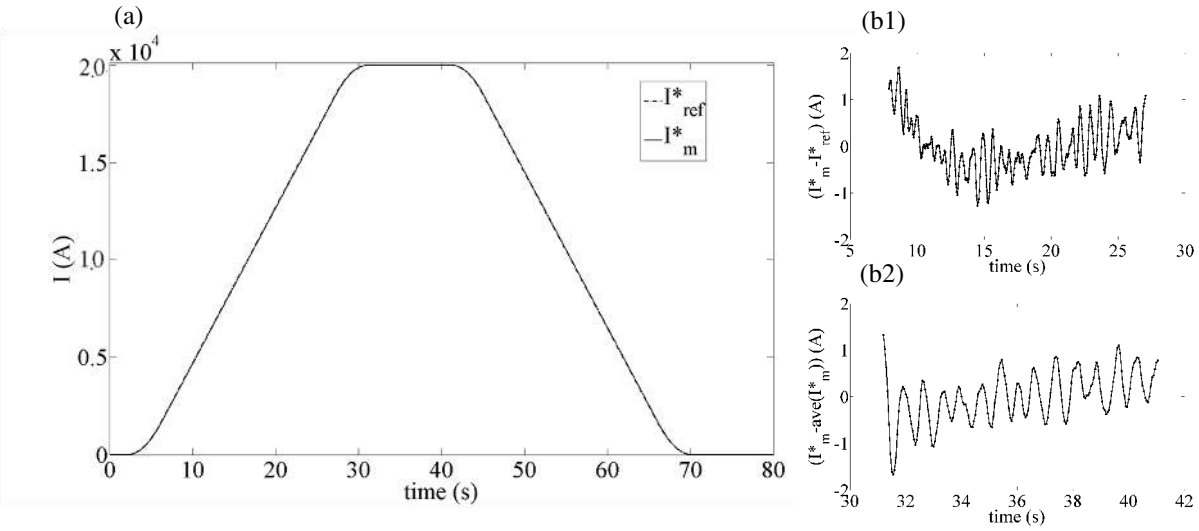

FIG. 11. Measured I^*_m and reference I^*_{ref} currents cycle at 20 kA (a), and differences between I^*_m and I^*_{ref} during ramp up (b1), and flattop with respect its average value (b2).

In all the cases of Tab. II, the ripple due to the controller is within ±1 A, either on the ramp-up or on the flattop, i.e. ±50 ppm of the maximum current 36 kA. The average current on the flattop differs from the ideal value by about 80 ppm. The control system largely meets the required low current noise and has satisfactory stability throughout the wide current range.

2. LHC cable of type 2 characterization

The proposed system was finally validated by testing an LHC outer layer dipole cable (LHC cable of type 2) [31]. The test generally consists in determining the voltage-current characteristic (also referred to as V-I curve), and defining the cable critical current at a criterion of resistivity of 10^{-14} Ohm m. This type of measurement has an expected repeatability of ±0.5 % and reproducibility of ±2 % [33]. A measurement campaign, with background field from 3.0 to 9.0 T, and current ramp rates from 50 to 800 As^{-1}, was carried out by using both the 32-kA power supply and the transformer. In addition, when using the transformer, long-term stability measurements were carried out in order to validate the findings on the low-level residual drift discussed earlier.

In Tab. III, the average values of the measured critical current on the sample under test with the reference 32-kA power supply and the superconducting transformer are compared by reporting also their percentage difference. The repeatability of the transformer system is ±0.5 %, and thus all the measurements of critical currents carried out by using both the systems are compatible.

TABLE.III Average critical current values.

Applied Field (T)	Transformer (A)	32kA Power supply (A)	Error (%)
3	22442 ± 49	22406	-0.16
4	18909 ± 94	18834	-0.40
5	15492 ± 20	15474	-0.12
6	12170 ± 55	12172	0.02
7	8808 ± 38	8782	-0.29
8	5468 ± 27	5498	0.56
9	2507 ± 16	2526	0.77

As an example, in Fig. 12, the measured V-I curves on a length of 610 mm of the cable are compared at 3.0 T and 6.0 T, with current ramp rate of 250 As^{-1}. The measured voltages overlap satisfactorily and the noise level is well inside the requirements. Indeed, the quality of the V-I curves measured by the proposed system is better than the one obtained using the 32-kA power supply.

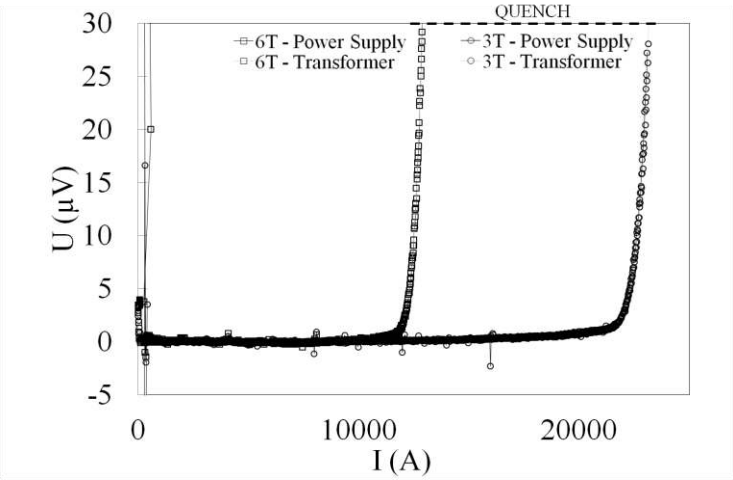

FIG. 12. Comparisons of U-I curves on a LHC cable of type 2 measured using the reference power supply and the superconducting transformer.

In Fig. 13, an example of a long-term stability tests is illustrated. A maximum current of 500 A, much less than the critical value of 14974 A, was kept on a long plateau, lasting 10 min. In particular, in Fig 13a, the current and the voltage for the central part of the cable in the insert are shown. The voltage measured on the sample has an inductive component,

visible during the current ramp. The voltage on the current plateau is higher than the initial value, at zero current, owing to a resistive contribution in the sample.

In Fig. 13b, the quantities measured during the flattop phase are shown on an enlarged scale. The noise level on the voltage sample lies within ±2 μV. The residual uncorrected drift on the current measurement turns out to be negligible for this long measurement. This result was verified on several other cycles by validating the high level of system stability.

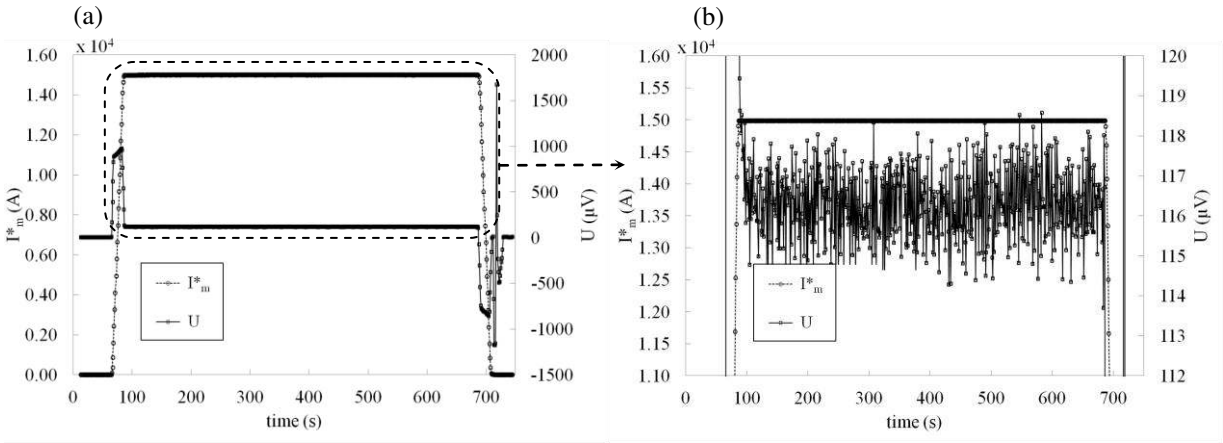

FIG. 13. Long-term stability tests: current and voltage on the cable (a), and detail of voltage along current plateau (b).

In Tab. IV, the final system performance such as experimentally determined are compared to the initial target requirements. Results are expressed in terms of typical and maximum performance attained during the overall test campaign. These specifications enable the system to achieve the results shown in this Section.

These results point out advancement in state-of-the-art measurement and control of secondary currents in superconducting transformers.

TABLE.IV Comparison of the proposed system requirements with experimental determinations.

	Requirement	Typical	Max
Current Measurement			
Resolution	3 A	1 A	#
Stability	$\pm$0.5 Amin^{-1}	$\pm$0.18 Amin^{-1}	$\pm$0.25 Amin^{-1}
Repeatability	$\pm$0.1%	$\pm$0.06%	$\pm$0.7%
Controller			
Ripple	0.01%	0.0025%	0.005%
Gain Error	100 ppm	60 ppm	80 ppm

IV. Conclusions

A fully digital system for the control of transformers for superconducting cable testing is proposed. The digital system is based on a low-drift precision integrator and a simple but robust PI control algorithm, achieving brilliant performance and improving test flexibility. The set-up has also a definite cost advantage for the use of off-the-shelf components.

The effectiveness of the architecture was assessed by an experimental implementation aimed at controlling the superconducting transformer available at the Facility for Research on Superconducting Cables (FReSCa) of CERN. Key performances achieved are an integrator residual drift below 0.25 $Amin^{-1}$ and a controller ripple less than ±50 ppm. These results were demonstrated in practical working conditions, measuring the critical current of a NbTi Rutherford cable with well known properties. The critical current measurements show full compatibility with the available reference system at FReSCa, by highlighting a quality of the V-I curves better than using the reference.

ACKNOWLEDGEMENTS

This work is supported by CERN trough the agreement TE/K1776 with the University of Sannio, whose support authors acknowledge gratefully. The authors thank F. Cennamo, L. Walckiers, S. Russenschuck, A. Ballarino, L. Fiscarelli, G. Peiro and G. Willering for their contribution, useful suggestions and cooperation.

References

[1] M. Leghissa *et al*., "Development and application of superconducting transformers", Physica C **372–376** (3), 1688 (2002).

[2] W. Buckel and R. Kleiner, *Superconductivity Fundamentals and Applications* (WILEY-VCH Verlag GmbH & Co. KGaA, Weinheim, 2004), p.269-302.

[3] P. Fabbricatore, R. Musenich, R. Parodi, "Inductive method for critical current measurement of superconducting cables for high energy physics applications", Nucl. Instrum. Methods **302** (1), 27 (1991).

[4] A.P. Verweij, J. Genest, A. Knezovic, D.F. Leroy, J.-P. Marzolf, L.R. Oberli, "1.9 K Test Facility for the Reception of the Superconducting Cables for the LHC", IEEE Trans. Appl. Sup., **9** (2), 153 (1999).

[5] C. Berriaud, S. Regnaud, L. Vieillard, "High Current Test Facility for Superconductors at Saclay", IEEE Trans. Appl. Sup. **11** (1), 3190 (2001).

[6] A.G. Prodell and A. Am,"A facility for Evaluating Superconductors above Atmospheric Pressure at 1.8K", Adv. Cryog. Eng. **43** (A), 443 (1998).

[7] H.H.J Kate ten, H.W. Weijers, J.M. Oort van, "Critical current degradation in Nb3Sn cables under transverse pressure", IEEE Trans. Appl. Sup. **3** (1), 1334, (1993).

[8] D.R. Dietderich, R.M. Scanlan, R.P. Walsh, and J.R. Miller, "Critical Current of Superconducting Rutherford Cable in High Magnetic Fields with Transverse Pressure". IEEE Trans. Appl. Sup. **2** (2), 122 (1999).

[9] J. Liu, Y. Wu, Zh. B. Ren, S. T. Wu, Y. Shi, J. Q. Peng, J. L. Chen, F. Long, M. Yu, and L. Qian, "Manufacturing of 50 kA superconducting transformer for ITER correction coil conductor test", Rev. Sci. Instrum. **81**, 044701 (2010).

[10] A. P. Verweij, C-H. Denarie, S. Geminian, O. Vincent-Viry, "Superconducting Transformer and Regulation Circuit for the CERN cable test facility", Proceedings of 7th European Conference on Applied Superconductivity, Vienna University of Technology, Austria, 2005, Journal of Physics Conference Series **43**, 833 (2006).

[11] A. Godeke *et al*., "A Superconducting Transformer System For High Current Cable Testing", Rev. Sci. Instrum. **81**, 035107 (2010).

[12] H.H.J. ten Kate, J.M. Mulders, J.L. de Reuver, and L.J.M. van de Klundert, "Ac Loss Measurements on a Superconducting Transformer for A 25 kA Superconducting Rectifier", Cryog. **8** (4), 439 (1984).

[13] J.L de Reuver, H.H.J. ten Kate, H.G. Knoopers and L.J.M. van de Klundert, "DC and AC Behaviour of a Normal Joint in a Superconducting Cable", Cryog. **5** (5), 251 (1984).

[14] N. Andreev *et al*., "Superconducting Current Transformer for Testing Nb3Sn Cable Splicing Technique", IEEE Trans. Appl. Sup. **13** (2), 1274 (2003).

[15] E. Barzi *et al*., "Study of Nb3Sn Cable Stability at Self-field using a Superconducting Transformer", IEEE Trans. Appl. Sup. **15** (2), 1537 (2005).

[16] E. Barzi *et al*., "Superconducting transformer for superconducting cable tests in a magnetic field", Transactions of the Cryogenic Engineering Conference, Tucson, Arizona, 2009, American Istitute of Physics Conference Proceeding **1218**, 421 (2010).

[17] P. Bruzzone *et al*.,"Status Report of the SULTAN Test Facility**",** IEEE Trans. Appl. Sup. **20** (3), 455 (2010).

[18] Kannan M. Moudgalys, *Digital Control* (Wiley, London, 2007).

[19] PXI Specification, http://www.pxisa.org/Specifications.html available on 12/11/2011.

[20] M. R. Aghaebrahimi and W. Menzies, "A Classical Approach in Modelling the Air-core Transformer" Proceedings of Communications Power and Computing Conference, Winnipeg, Manitoba, 1997, IEEE WESCANEX97 Proceedings, 344 (1997).

[21] Yi Shi, Yu Wu, Songtao Wu, Huajun Liu, and Jinqing Peng, "The 50 kA Superconducting Transformer for Testing ITER CC Conductors Short Sample", IEEE Trans. Appl. Sup. **20** (3), 1155 (2010).

[22] NI-PXI 628, http://sine.ni.com/nips/cds/view/p/lang/en/nid/14119 available on 12/11/2011.

[23] T. Boutboul, C.-H. Denarié, Z. Charifoulline, L. Oberli and D. Richter, "Critical Current Test Facilities For LHC Superconducting NbTi Cable Strands", 5th European Conference on Applied Superconductivity, Lyngby, Denmark, 2001, **1**, 8 (2001).

[24] Model 620/622/647, http://www.lakeshore.com/downloads.html available on 12/11/2011.

[25] P. Arpaia, A. Masi, and G. Spiezia, "Digital Integrator for Fast Accurate Measurement of Magnetic Flux by Rotating Coils", IEEE Trans. Instrum. Meas. **56** (2), 216 (2007).

[26] NI PXI-6682, http://sine.ni.com/nips/cds/view/p/lang/en/nid/203944 available on 12/11/2011.

[27] Agilent Acqiris 3-, 5-, and 8-Slot cPCI Crates, http://cp.literature.agilent.com/litweb/pdf/U1092-90018.pdf available on 12/11/2011.

[28] D9 - 6U, http://www.men.de/products/02D009-.html#t=overview available on 12/11/2011.

[29] P. Arpaia *et al*., "A Flexible Framework for generating Magnetic Measurement Automatic Systems at CERN", Procceding of IEEE Instrumentation and Measurement Technology Conference, Warsaw, Poland, 2007, 1 (2007).

[30] J. F. James, *A Student's Guide to Fourier Transforms : With Applications in Physics and Engineering* (Cambridge University Press, Cambridge, 2011), p. 1-39.

[31] T. Shimada *et al*., "Manufacturing of Superconducting Cable for the LHC - Key Technology and Statistical Analysis", IEEE Trans. Appl. Sup. **12** (1), 1075 (2002).

[32] P. Burla , Q. King, and J.G. Pett, "Optimisation of the Current Ramp for the LHC", Proceedings of the 1999 Particle Accelerator Conference, New York, USA, 1999, **2**, 762 (1999).

[33] A. P. Verweij and A. K. Ghosh, "Critical Current Measurements of the Main LHC Superconducting Cables", IEEE Trans. Appl. Sup. **17** (2), 1454 (2007).